the junction of two parts, such as sharp connecting corners in Fig. 12.7, stimulus 1, are also not essential. We recorded single-cell responses from a spot having stimulus selectivity described above, and found three characteristic response properties ($n = 14$):

(1) These cells had critical features which were combinations of two vertically aligned parts (Fig. 12.8a, see also Fig. 12.1). There was no activation by either part (Fig. 12.1, step 4).

(2) These cells were less sensitive to color, texture, and local shapes of either part. Three findings suggest this conclusion. First, there were no changes in the responses after removing color and texture during the stimulus simplification procedure (Fig. 12.1 and 12.8a). Secondly, changes in the shapes of the parts did not alter responses of these neurons very much. For example, a neuron, whose critical feature was determined as a combination of a circle and a rectangle, was also significantly activated by a combination of a circle and an ellipse (data not shown). Finally, these cells responded equally well to object images even having different color, texture, and local shapes, as long as they had the global shape similar to the critical features (Figs 12.8b and 12.9).

(3) These cells were highly selective to a particular position of the upper part relative to the lower part (Fig. 12.10).

These characteristic response properties enable these neurons to respond to visual stimuli regardless of the local features embedded in either part, but only when these local features are aligned in particular orientation, as in Fig. 12.10. These results, as well

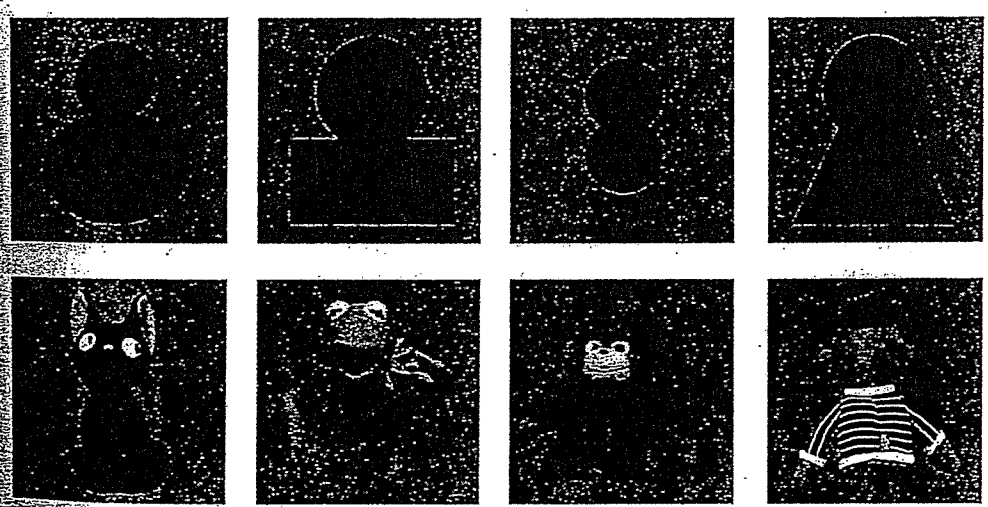

Fig. 12.8 Effective stimuli for neurons in a spot identified by the stimuli in Fig. 12.7. (a) Representative critical features determined by stimulus simplification. Please note that, when color and texture are not essential, the stimulus was filled black (see Fig. 12.1). (b) The best object stimuli for these neurons, among 100 object stimuli examined before stimulus simplification. Scale bar, 5°.

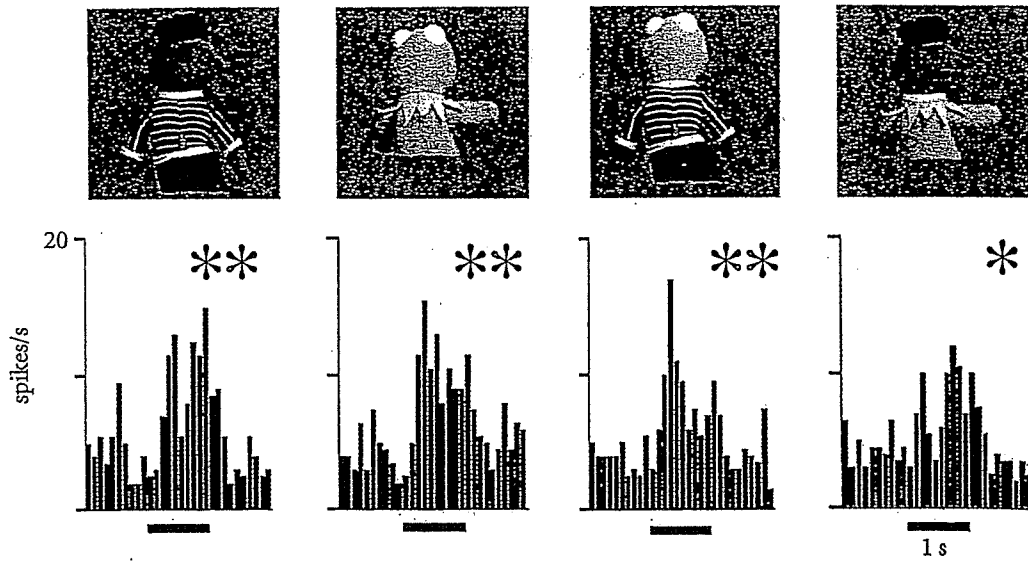

Fig. 12.9 Neural responses of one representative neuron to object stimuli. Upper panel shows visual stimuli, and lower panel indicates peristimulus–time histograms (PSTHs) showing responses of the neuron to the stimuli given above. The stimulus was presented for a period of 1 s, indicated by the horizontal line segment in each PSTH. These stimuli activated the cell equally well. $*P < 0.05$, $**P < 0.01$.

as neurons in spot C in Fig. 12.4b, suggest that neurons in area TE do not necessarily represent local features but also configurational information of the object image. Object images could be specifically represented by a combination of spots representing 'local features' and those representing 'configurational information'.

12.7 Face-specific neurons in area TE

'Face neurons' are representative neurons in area TE responding to the visual images of familiar objects. We consider that 'face neurons' also represent 'configurational information'. 'Face neurons' respond to 'faces', but these responses cannot be explained by specific responses to a part of the 'face' (Fig. 12.11). In this particular case, for example, a face without eyes did not activate the cell, but there was no activation by 'eyes' alone (Fig. 12.11b, c). Furthermore, previous studies have shown that a 'face' with scrambled facial parts does not activate these neurons (Desimone *et al.* 1984). There are two characteristic properties of 'face neurons'. First, many of them are broadly tuned to images of faces from a particular vantage point (Fig. 12.11a; Desimone *et al.* 1984; Perrett *et al.* 1991). Secondly, these cells have sensitivity to individual faces, but the tunings are broad (Perrett *et al.* 1984; Baylis *et al.* 1985; Yamane *et al.* 1988; Young and Yamane 1992). These response properties suggest that face neurons represent the 'configuration' specific to faces.

Intrinsic signal imaging showed that there are spots specifically activated by faces (Wang *et al.* 1996, 1998) (Fig. 12.12). Thus, face neurons, as well as neurons specifically

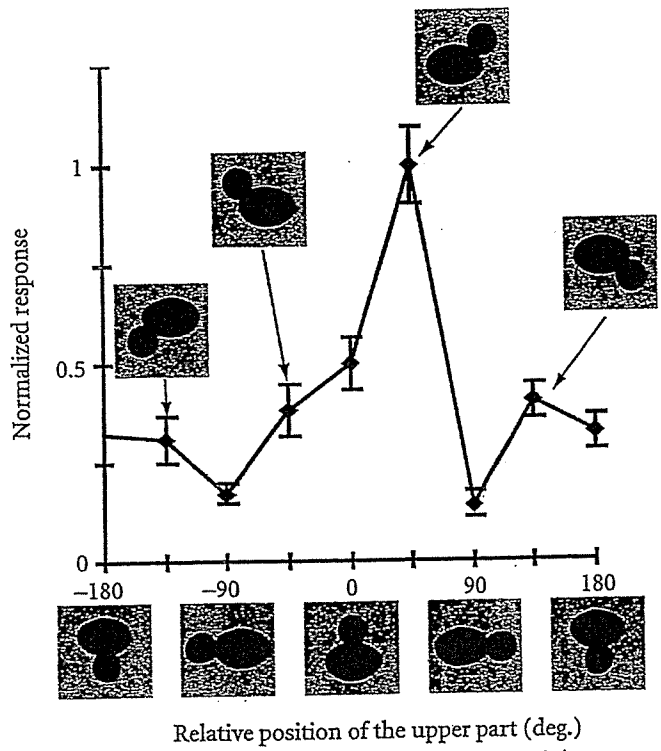

Fig. 12.10 Response specificity of a representative cell to the spatial arrangement of parts. The upper part of the critical feature of the cell was rotated relative to the lower part. The horizontal axis indicates the angle between the line connecting the center of upper and lower parts of each stimulus and that of the critical feature. The vertical axis indicates normalized value of stimulus evoked responses. In this particular case, the best response was elicited by the stimulus with 45°, but this is not only the case. Some other neurons respond maximally at 0°. It may be the case that neurons with different angles are located in close vicinity, as is the case for face columns (Fig. 12.12).

responding to visual features, are clustered together. Furthermore, activation patterns produced by images of faces from different vantage points revealed that the peaks of activity spots shift along the cortical surface as the face rotates from the left profile, to the right profile, through the front face. This representation of faces from different vantage points in close vicinity may be important for view-independent recognition of faces.

12.8 Summary and conclusions

In summary, our results from both optical and extracellular recordings provide evidence that a complex object is represented by combinations of columns in area TE, each of which represents visual features of the object image. The combinations are not simply based on summing up of the columns, but may instead rely on a combination of active and inactive columns to represent objects. These columns do not necessarily

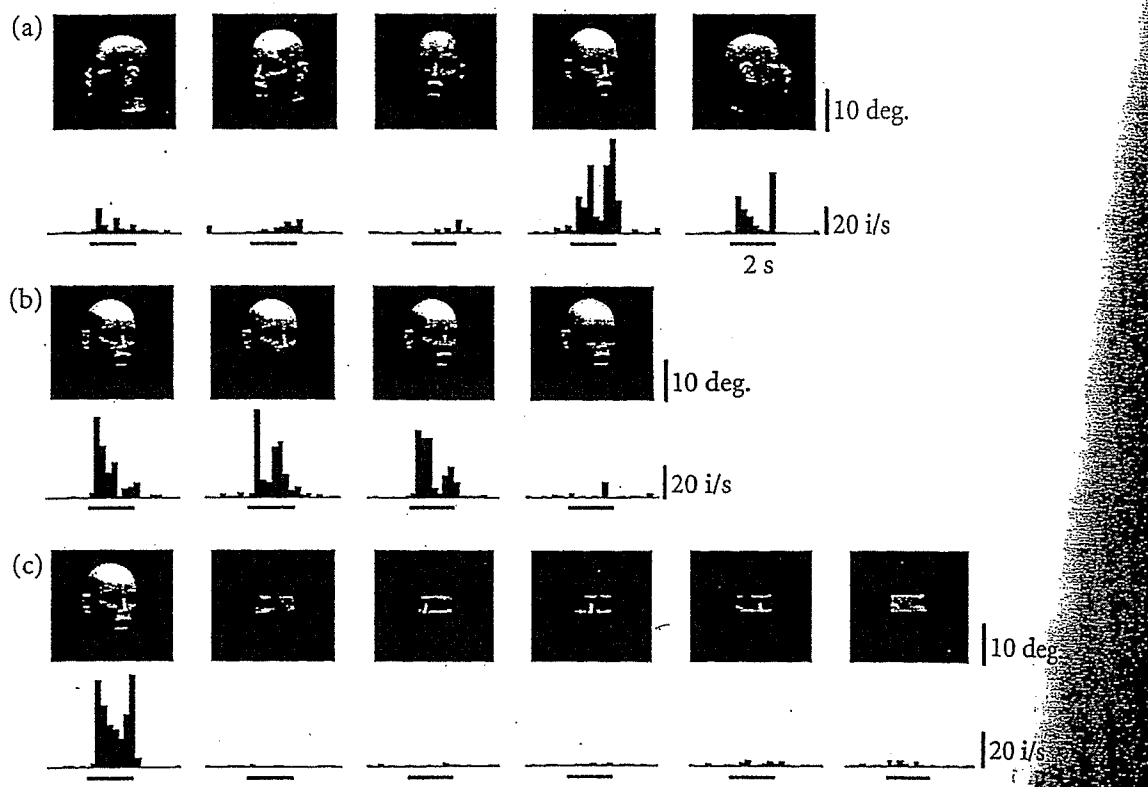

Fig. 12.11 Response properties of a typical face neuron shown by the PSTHs of neural responses evoked by stimuli given above. The recording consisted of three sessions. In the first session, (a), we examined selectivity of the neuron to a face at different vantage points. In the second session, (b), we examined the same neuron with face stimuli lacking different parts of the face. In the final session, (c), we examined responses to insolated eyes from different vantage points.

represent 'local features' but some of them may represent visual features related to 'configurational information'. We consider that neurons specific for images of familiar objects, such as 'faces', also represent visual features specific for these objects. For example, face neurons may represent 'configuration' specific for 'faces'. An image of a particular face could be represented by a combination of columns. Some of the columns represent 'local feature' specific to an individual, and others represent configurational information about the face at a particular vantage point.

Visual features represented in area TE seem to range from simple features such as 'rectangular shape' to highly complex visual features such as 'configuration of face'. Although there is no direct evidence, this wide range of complexity in visual features may be produced through experience-dependent association of visual features. For example, neurons responding to vertically aligned parts (Fig. 12.8) may be generated because monkeys frequently experience objects having such a part arrangement. In support, in monkeys trained with a particular set of visual stimuli, previous studies revealed that some neurons specifically responded to visual stimuli that became

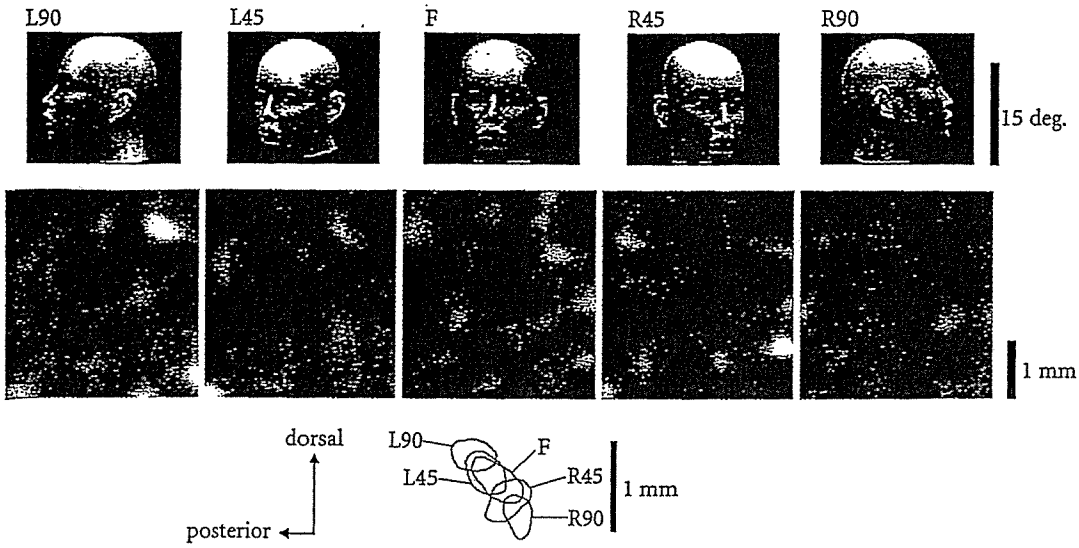

Fig. 12.12 Systematic shift of activation spots with rotation of the face. Images of the same cortical area (middle panels) obtained for five different views of the same mannequin face (top panels). The contours of the activity spots are superimposed at the bottom. (Adapted from Wang *et al.* 1996 Permission sought.)

through training (Logothetis *et al.* 1995; Kobatake *et al.* 1998). Those visual stimuli could represent 'local features' or 'configurational information' depending on the stimulus set and the task design.

Acknowledgements

We thank R. Uma Maheswari, Kathleen Rockland, and Charles Rockland for helpful comments on the manuscript. This work was partly supported by Research Fellowships of the Japan Society for the Promotion of Young Scientists to Y.Y.

References

Baylis, G.C., Rolls, E.T., and Leonard, C.M. (1985) Selectivity between faces in the responses of a population of neurons in the cortex in the superior temporal sulcus of the monkey. *Brain Res.* 342, 91–102.

Desimone, R., Albright, T.D., Gross, C.G., and Bruce, C. (1984) Stimulus-selective properties of inferior temporal neurons in the macaque. *J. Neurosci.* 4, 2051–62.

Field, P. and Young, M.P. (1995) Sparse coding in the primate cortex. In M.A. Arbib (ed.) *The handbook of brain theory and neural networks* (pp. 895–8). MIT Press, Cambridge MA.

Fujita, I. and Fujita, T. (1996) Intrinsic connections in the macaque inferior temporal cortex. *J. Comp. Neurol.* 368, 467–86.

Fujita, I., Tanaka, K., Ito, M., and Cheng, K. (1992) Columns for visual features of objects in monkey inferotemporal cortex. *Nature* 360, 343–6.

Gochin, P.M., Miller, E.K., Gross, C.G., and Gerstein, G.L. (1991) Functional interactions among neurons in inferior temporal cortex of the awake macaque. *Exp. Brain Res.* 84, 505–16.

Grinvald, A., Shoham, D., Shmuel, A., Glaser, D., Vanzetta, I., Shtoyerman, E., Slovin, H., Wijnbergen, C., Hildesheim, R., and Arieli, A. (1999) In-vivo optical imaging of cortical architecture and dynamics. In U. Windhorst and H. Johansson (Eds.), *Modern techniques in neuroscience research* (pp. 893–970). Springer, Berlin.

Gross, C.G., Rocha-Miranda, C.E., and Bender, D.B. (1972) Visual properties of neurons in inferotemporal cortex of the Macaque. *J. Neurophysiol.* 35, 96–111.

Kisvarday, Z.F., Kim, D-S., Eysel, U.T., and Bonhoeffer, T. (1994) Relationship between lateral inhibitory connections and the topography of the orientation map in cat visual cortex. *Eur. J. Neurosci.* 6, 1619–32.

Kobatake, E. and Tanaka, K. (1994) Neuronal selectivities to complex object features in the ventral visual pathway of the macaque cerebral cortex. *J. Neurophysiol.* 71, 856–67.

Kobatake, E., Wang, G., and Tanaka, K. (1998) Effects of shape-discrimination training on the selectivity of inferotemporal cells in adult monkeys. *J. Neurophysiol.* 80, 324–30.

Logothetis, N.K., Pauls, J., and Poggio, T. (1995) Shape representation in the inferior temporal cortex of monkeys. *Curr. Biol.* 5, 552–63.

Malach, R., Reppas, J.B., Benson, R.R., Kwong, K.K., Jiang, H., Kennedy, W.A., Ledden, P.J., Brady, T.J., Rosen, B.R., and Tootell, R.B. (1995) Object-related activity revealed by functional magnetic resonance imaging in human occipital cortex. *Proc. Natl Acad. Sci. USA* 92, 8135–39.

Perrett, D.I., Rolls, E.T., and Caan, W. (1982) Visual neurones responsive to faces in the monkey temporal cortex. *Exp. Brain Res.* 47, 329–42.

Perrett, D.I., Smith, P.A.J., Potter, D.D., Mistlin, A.J., Head, A.S., Milner, A.D., and Jeeves, M.A. (1984) Neurons responsive to faces in the temporal cortex: studies of functional organization, sensitivity to identity and relation to perception. *Hum. Neurobiol.* 3, 197–208.

Perrett, D.I., Oram, M.W., Harries, M.H., Bevan, R., Hietanen, J.K., Benson, P.J., and Thomas, S. (1991) Viewer-centered and object-centered coding of heads in the macaque temporal cortex. *Exp. Brain. Res.* 86, 159–73.

Saleem, K.S., Tanaka, K., and Rockland, K.S. (1993) Specific and columnar projection from area TEO to TE in the macaque inferotemporal cortex. *Cerebr. Cortex* 3, 454–64.

Tanaka, K., Saito, H., Fukada, Y., and Moriya, M. (1991) Coding visual images of objects in the inferotemporal cortex of the macaque monkey. *J. Neurophysiol.* 66, 170–89.

Tsunoda, K., Yamane, Y., Nishizaki, M., and Tanifuji, M. (2001) Complex objects are represented in macaque inferotemporal cortex by the combination of feature columns. *Nat. Neurosci.* 4, 832–8.

Wang, G., Tanaka, K., and Tanifuji, M. (1996) Optical imaging of functional organization in the monkey inferotemporal cortex. *Science* 272, 1665–8.

Wang, G., Tanifuji, M., and Tanaka, K. (1998) Functional architecture in monkey inferotemporal cortex revealed by in vivo optical imaging. *Neurosci. Res.* 32, 33–46.

Yamane, S., Kaji, S., and Kawano, K. (1988) What facial features activate face neurons in the inferotemporal cortex of the monkey? *Exp. Brain. Res.* 73, 209–14.

Yamane, Y., Tsunoda, K., Matsumoto, M., Phillips, A., and Tanifuji, M. (2001) Decomposition of object images by feature columns in macaque inferotemporal cortex. *Neurosci. abstr* 399.6.

Young, M.P. and Yamane, S. (1992) Sparse population coding of faces in the inferotemporal cortex. *Science* 256, 1327–31.

Human Molecular Genetics, 2005, Vol. 14, No. 6 735–745
doi:10.1093/hmg/ddi069
Advance Access published on January 27, 2005

The *Pax6* isoform bearing an alternative spliced exon promotes the development of the neural retinal structure

Noriyuki Azuma[1,2,*], Keiko Tadokoro[2], Astuko Asaka[2], Masao Yamada[2], Yuki Yamaguchi[3], Hiroshi Handa[3], Satsuki Matsushima[4], Takashi Watanabe[4], Shinichi Kohsaka[5], Yasuyuki Kida[6], Tomoki Shiraishi[6], Toshihiko Ogura[6], Kenji Shimamura[7,8] and Masato Nakafuku[7,9]

[1]Department of Ophthalmology, National Center for Child Health and Development, Tokyo 157-8535, Japan, [2]Department of Genetics, National Research Institute for Child Health and Development, Tokyo 154-8567, Japan, [3]Department of Biological Information, Tokyo Institute of Technology, Graduate School of Bioscience and Biotechnology, Yokohama, 226-8501, Japan, [4]Department of Laboratory Medicine, Kyorin University School of Medicine, Tokyo 181-8611, Japan, [5]National Institute of Neuroscience, Tokyo 187-8502, Japan, [6]Department of Developmental Neurobiology, Institute of Development, Aging and Cancer, Sendai 980-8575, Japan, [7]Department of Neuroscience, University of Tokyo Graduate School of Medicine, Tokyo 113-0033, Japan, [8]Division of Morphogenesis, Department of Embroyogenesis, Institute of Molecular Embryology and Genetics, Kumamoto University, Honjo 2-2-1, Kumamoto 860-0811, Japan and [9]Division of Developmental Biology, Cincinnati Children's Hospital Research Foundation, Cincinnati, OH 45229, USA

Received November 28, 2004; Accepted January 18, 2005

The vertebrate retina has an area where visual cells are closely packed for proper vision that is known as a fovea, an area centralis or a visual streak. The molecular mechanism that regulates the formation of these structures and visual cell gradients is unknown. The transcription factor Pax6 is a master regulator of eye development. A Pax6 isoform that contains an exon 5a-encoded 14 amino acid insertion in its paired domain, Pax6(+5a), has different DNA-binding properties compared with the Pax6(−5a) isoform. Little is known about the functional significance of Pax6(+5a). Here, we show that Pax6(+5a) is expressed especially in the retinal portion where visual cells accumulate during eye development and, when overexpressed, induces a remarkable well-differentiated retina-like structure. Pax6(+5a) proteins that bear point mutations that are found in patients with foveal hypoplasia are unable to induce these ectopic retina-like structures. We propose that Pax6(+5a) induces a developmental cascade in the prospective fovea, area centralis or visual streak region that leads to the formation of a retinal architecture bearing densely packed visual cells.

INTRODUCTION

Most vertebrates have a region of the retina where cone photoreceptors, bipolar cells and ganglion cells accumulate and specialize, which contributes to better vision (1–3). This region comes in two general forms, namely, a visual streak and an area centralis. Animals that are nocturnal or have relatively poor vision bear a visual streak, where the photoreceptors, bipolar cells and ganglion cells congregate and become specialized along a horizontal line of the eye fundus. In contrast, animals that have relatively good vision bear the area centralis, which is a circular spot in the retina. The image of an object becomes centered on this region. A specialized form of the area centralis is the fovea, which helps many reptiles and birds, and most primates achieve greater visual sensitivity. The fovea is an area in which cone photoreceptors are highly concentrated and the inner retina is thinned. Human patients lacking the fovea have a poor visual acuity of 0.1–0.3, even with lens correction (4,5). Thus, the fovea

*To whom correspondence should be addressed at: Department of Ophthalmology, National Center for Child Health and Development, 2-10-1 Okura, Setagaya-ku, Tokyo 157-8535, Japan. Tel: +81 334160181; Fax: +81 334162222; Email: azuma-n@ncchd.go.jp

is an essential architectural feature that is required for our sharp visual acuity.

In most vertebrates that have a fovea or an area centralis, the retinal cells first accumulate, differentiate and form synaptic connections at the prospective fovea or area centralis region during the very early stages of eye development, corresponding to the time when ganglion cells appear in the retina. The differentiation of the retinal cells then progresses from the centre to the periphery, which results in a gradient of visual sensitivity (2,3). The molecular mechanisms that regulate the formation of these specific retinal structures are not well elucidated, although previous studies have explored mechanism and genes involved in differentiation of the retinal area (6–8).

Recently, patients with foveal hypoplasia were found to bear mutations in the *PAX6* gene (4,5). The *Pax6* gene encodes a transcription factor and plays important roles in eye morphogenesis in both vertebrates and invertebrates (9–12). This gene has been reported to induce ectopic eye formation in *Drosophila melanogaster* (13) and *Xenopus* larvae (14), and is known as a master control gene in eye formation (9–11). Pax6 is expressed in various eye tissues. In the neural retina, Pax6 is expressed widely in multipotent progenitor cells at early stages and to a lesser extent in ganglion, horizontal and amacrine cells at late stages (15–17). The *Pax6* gene produces two isoforms by alternative splicing, namely, Pax6(−5a) and Pax6(+5a). Pax6(+5a) differs from Pax6(−5a) by the presence of an exon 5a-encoded 14 amino acid insertion in its paired-type DNA-binding domain (paired domain, or PD) (18,19). Pax6(−5a) and Pax6(+5a) show distinct DNA-binding properties (20) and their distinct consensus binding sequences have been determined. These are termed P6CON and 5aCON, respectively (21). Mutational analyses have shown that the N-terminal subdomain (NTS) and the C-terminal subdomain (CTS) of the Pax6 PD are respectively responsible for the DNA-binding abilities of Pax6(−5a) and Pax6(+5a) and their transactivation activity (20,22). Pax6(−5a) binds to a promoter element of the *ζ-crystallin* gene at a site that is highly similar to P6CON (23), while target genes of Pax6(+5a) that bear 5aCON-like sequences are yet to be identified.

Many mutations in the *PAX6* gene have been identified in human patients with foveal hypoplasia (4,5,24–27). In most classical aniridia patients, caused by haploinsufficiency of PAX6 due to its deletion or the presence of a nonsense mutation, all other eye tissues apart from the iris, including the cornea, lens, fovea and optic nerve, are also affected. In contrast, missense mutations in the *PAX6* gene cause more specific eye anomalies (4,5,25–27), probably because Pax6 has multiple functional domains and that missense mutations in this gene disturb one or only a few of these domains. Previously, we reported two PAX6 missense mutations, R128C in the CTS of the PD and V54D in exon 5a, in Japanese patients with foveal hypoplasia (4,5). An R128C mutation was again identified in an independent European patient with the same phenotype (26). These findings suggest that the CTS and exon 5a, which are two elements that are thought to be important for the function of the Pax6(+5a) isoform, may be involved in the formation of the fovea. We investigated expression pattern of Pax6(+5a) in the developing retina and effect of the isoform in retinal development by gain-of-function experiments, and here present evidence that Pax6(+5a) contributes to promote the formation of the retinal structure.

RESULTS

Pax6(+5a) is abundantly expressed in the retinal portion where visual cells accumulate

We first examined the regional expression of the Pax6 isoforms by subjecting sections of a neonatal marmoset eye (which has a fovea) to immunohistochemical staining with two different antibodies that can distinguish between the two Pax6 isoforms. One of these antibodies, which is denoted as anti-Pax6, was raised against amino acids 1–223 including those encoded by exon 5a. This antibody reacts with both Pax6(−5a) and Pax6 (+5a), as reported previously (16,17). For this study, we raised another antibody against a synthetic peptide consisting of the 14 amino acid residues that are encoded by exon 5a (anti-exon 5a). Western blotting of proteins prepared from cultured mouse embryonic carcinoma P19 cells that had been transfected with constructs expressing Pax6(−5a) or Pax6(+5a), and of marmoset tissues expressing both isoforms demonstrated the specificity of these antibodies (Fig. 1A). On the marmoset sections, anti-Pax6 visualized three layers, namely, the ganglion cell layer and the inner and outer edges of the inner nuclear layer of the retina. The foveal region was heavily stained, and both the nasal and temporal nasal sides were also stained (Fig. 1C, middle panels). This indicates the wide distribution of Pax6 proteins throughout the entire retina. In contrast, the anti-exon 5a staining pattern suggested that the Pax6(+5a) protein localizes to a restricted retinal area between the optic nerve head and the fovea (Fig. 1C b and c). This was clear when the staining in the nasal and foveal sides of the optic nerve head was compared. The staining was identified scarcely in the nasal side but obviously in the foveal side (Fig. 1C b). From these observations, we conclude that the Pax6(+5a) isoform is expressed especially in the restricted retinal portion where the densely packed visual cells reside.

Reflecting evolutionary conservation of the amino acid sequence encoded by exon 5a, the anti-exon 5a antibody reacts with chicken Pax6(+5a) as well, albeit weakly. In the chicken retina of Hamburger–Hamilton (HH) stage 45, the Pax6(+5a) protein appears to localize in a restricted retinal area of the visual streak, whereas the Pax6(−5a) protein distributes throughout the entire retina (Fig. 2A). To compare the expression levels of the two isoforms, we next performed semi-quantitative RT–PCR analysis using dissected retinal tissues of chick embryos at HH stages 12–45. The isolated RNAs were subjected to RT–PCR analysis using specific primers that flank exon 5a and can distinguish between the two isoforms *Pax6(+5a)* and *Pax6(−5a)*. At an early developmental stage (HH stage12), when the optic vesicle is formed and multipotent progenitor cells still exist in the neural retina, the two isoforms were expressed in both the central nervous system (CNS) and the eye primordium but the *Pax6(−5a)* isoform predominated (Fig. 2B). At HH stage 20, Pax6(−5a) was still the major transcript. At this stage, the formation of the eye is proceeding and lens

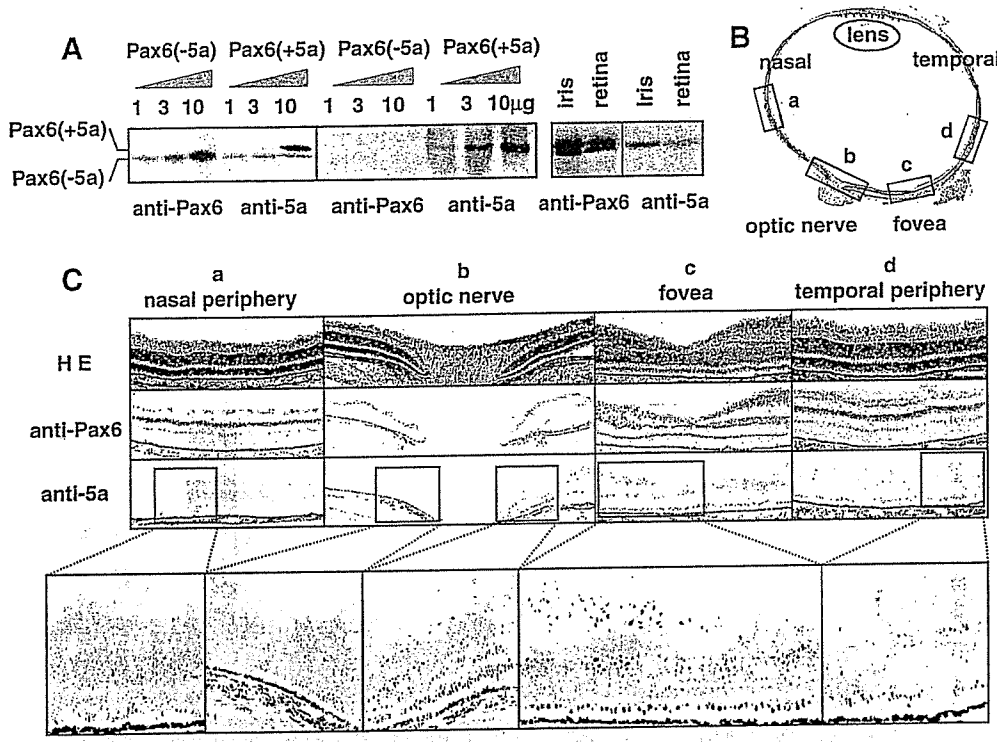

Figure 1. Histochemical analysis of the expression of the two Pax6 isoforms in the neonatal marmoset eye. (**A**) Western blotting analysis confirming the specificity of the two antibodies that were used. P19 cells (10^5 cells) were transfected with either the Pax6(−5a) or Pax6(+5a) expression construct and nuclear protein fractions obtained 24 h post-transfection were analyzed. Anti-Pax6 recognized the exogenously expressed Pax6(−5a) and Pax6(+5a) proteins as well as endogenous Pax6(−5a) protein, whereas anti-exon 5a recognized Pax6(+5a) but not Pax6(−5a). Western blotting analysis of nuclear fraction proteins obtained from the iris and retina tissues of the neonatal marmoset (*Callithrix jacchus*) also showed that anti-Pax6 recognized both native Pax6(−5a) and Pax6(+5a) proteins, whereas anti-exon 5a recognized Pax6(+5a) but not Pax6(−5a). (**B**) View of a horizontal section of the eye of a neonatal marmoset stained with HE. (**C**) Magnified fields of the eye stained with HE, anti-Pax6 or anti-exon 5a (bar scale 100 μm). Further enlarged images are shown below. a, nasal peripheral area; b, optic nerve head area; c, fovea area; d, temporal peripheral area. The staining for anti-exon 5a localizes around the fovea area, whereas that for anti-Pax6 is detected throughout the entire retina. The result shown is representative of three independent experiments using four marmoset eyes.

formation is evident. During HH stages 24–30, the ganglion cells in the retina differentiate. The level of *Pax6(−5a)* expression seems to decrease transiently at HH stage 24 and increase at HH stage 30. Interestingly, the level of *Pax6(+5a)* expression gradually increased during this period in all ocular tissues such as the cornea, lens and retina. Increased expression of *Pax6(+5a)* was also evident in the retina in later stages (HH stages 36–45), when all photoreceptors, horizontal and amacrine cells differentiate. Although the eyes of domestic birds lack the fovea, they possess a distinct visual streak in the posterior portion of the retina (1,2). Expression of *Pax6(+5a)* became particularly intense in this posterior portion. At HH stage 36, the expression of *Pax6(+5a)* exceeded that of *Pax6(−5a)* in the posterior retina. These observations indicate that expression of the two Pax6 isoforms are differentially regulated during retinal development, with Pax6(+5a) expression increasing only in a specified region, whereas Pax6(−5a) expression being throughout the retina.

In *ovo* misexpression of *Pax6(+5a)* gene markedly expands the retinal layer and promotes the growth and differentiation of retinal cells into visual cells

Next, we investigated the roles the two Pax6 isoforms play in the formation of the eye architecture by *in ovo* electroporation (28). Thus, an expression construct for either Pax6(+5a) or Pax6(−5a) was electroporated into the developing retina of HH stages 16–30 chick embryos, together with an expression construct of green fluorescence protein (GFP) (29) to monitor the expression of the transgenes. Expression plasmids [pCAGGS-PAX6(−5a) and pCAGGS-PAX6(+5a)] carry the entire human *PAX6* coding region with or without exon 5a under the control of a cytomegalovirus enhancer and chicken β-actin promoter, as described previously (5,22). Embryos that had been electroporated were harvested at various stages and analyzed. Retinal formation was scarcely affected when either isoform was transduced after HH stage 30 (data not shown). However, marked changes were observed when either isoform was transduced at HH stages 16–24, when the formation of the optic cup was completed. Six to twelve hours after electroporation of Pax6(−5a) and GFP (HH stage 18), the electroporated region, confirmed by staining with anti-Pax6 and anti-GFP antibodies, was found to proliferate excessively, as evidenced by intense staining with anti-5-bromo-2′-deoxyuridine (BrdU) antibody (Fig. 3). The promotion of retinal cell proliferation occurred similarly up to this stage regardless of the Pax6 isoforms overexpressed (data not shown). Electroporation of the empty vector alone, the pCAGGS-GFP or both constructs did not induce any change.

At later stages, a significant difference in the effect of the two Pax6 isoforms was observed. When Pax6(−5a) was

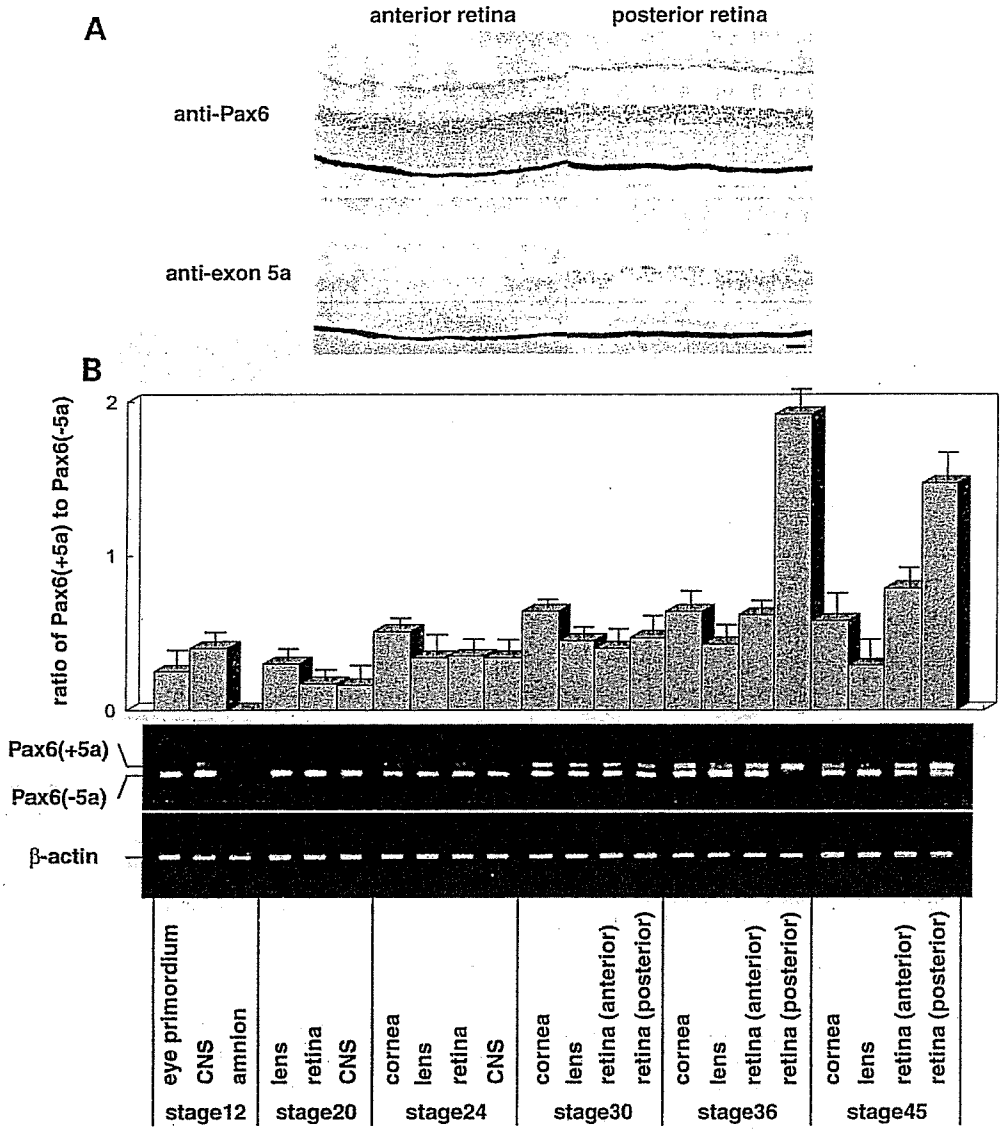

Figure 2. (**A**) Horizontal sections of the chick eye at HH stage 45 stained with anti-Pax6 or anti-exon 5a antibody (bar scale 20 μm). The Pax6(+5a) protein appears to localize in the posterior retina containing the visual streak, whereas the Pax6(−5a) protein distributes throughout the entire retina. (**B**) Semi-quantitative RT–PCR analysis of the expression of the two *Pax6* isoforms in developing chick embryos. As the eye became big enough to be dissected at later stages, *Pax6* expression could be examined in particular parts of the eye structure. The indicated PCR fragments were judged to represent one or the other *Pax6* isoform by their sizes. This was confirmed by sequencing. In the posterior retina, tissues were excised from the visual streak region. Amnion tissues were used as a negative control for *Pax6* expression and *β-actin* represents the amounts of RNA in each lane. The bar graph is shown as mean ± SD ($n = 3$) of expression ratio of Pax6(+5a) to Pax6(−5a). The photograph of RT–PCR analysis under the bar graph is representative of three independent experiments.

misexpressed, 3–7 days after the electroporation (HH stages 28–35), 47% ($n = 198$) of the eyes were larger than the untreated control eyes (Fig. 4A). Several isolated swelling spots (bulges) or lines (wrinkles) on the retina were observed in 68% of the 198 treated eyes. Green fluorescence was also observed at these areas (Fig. 4B). Histological examination showed that the retina was thickened. Sections were stained with specific antibodies for Islet1, a homeodomain-containing transcription factor that is expressed in the ganglion cells in the developing retina (30), and neurofilament protein, an intermediate filament protein specific to retinal neurons (31). The immunohistochemistry revealed that the differentiation of ganglion cells had expanded to the surface layer at these places (Fig. 4C). In 32% ($n = 198$) of the Pax6(−5a)-treated eyes, an embankment-like structure swelled out on the retina. In addition, several fibres (10–100 μm in length) grew out into the vitreous cavity (Fig. 4D). The immunohistochemistry with anti-Islet1 and anti-neurofilament antibodies suggested that the fibres in the vitreous cavity were nerve bundles derived from ganglion cells (Fig. 4E). These abnormal structures may be caused by the unbalanced growth and differentiation of the retina, because the nerve fibres extended onto the retinal surface and formed additional layers on the retina.

When the Pax6(+5a) isoform was misexpressed instead of Pax6(−5a), more dramatic changes were observed inside the enlarged eyes 3–7 days after electroporation (HH stages

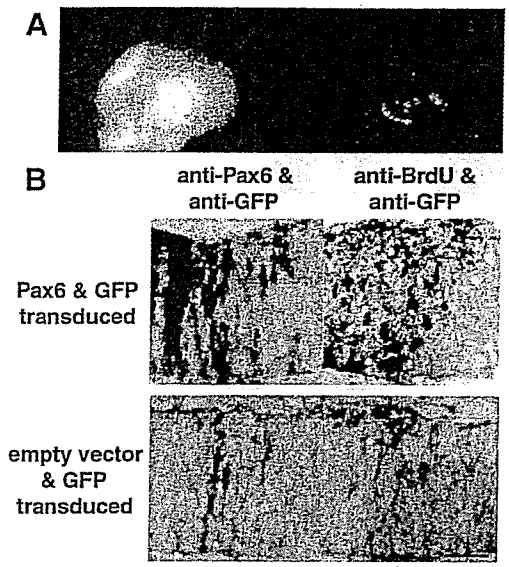

Figure 3. Early changes in the developing chick eye induced by the electroporation of Pax6(−5a). Constructs expressing Pax6(−5a) and GFP were electroporated into the right eye primordium of HH stage 16 chick embryos ($n = 5$). (**A**) Twelve hours after electroporation (HH stage 18), expression of GFP in the right eye was examined using fluorescence microscopy. (**B**) Sections double-immunostained with anti-GFP (violet) and anti-Pax6 (brown) and anti-GFP (violet) and anti-BrdU (brown) antibodies show the expression of the electroporated GFP and Pax6(−5a) constructs and the pronounced proliferation of the retinal progenitor cells around the electroporated area, but transduction of empty vector, pCAGGS-GFP or both constructs did not induce any change ($n = 5$ for each). (bar scale 20 μm). Transduction of the Pax6(+5a) isoform had a similar effect on eye development at these stages ($n = 5$; data not shown).

28–35). Of the 187 treated eyes, 6% had a wall-like structure protruding into the vitreous cavity, which was shown to be a folded retina by histological analysis (Fig. 4G and H) and 42% showed thick stick-like structures protruding from the retina into the vitreous cavity (Fig. 4I and J). These protruding structures were very long and some even approached the lens on the opposite side. Cross sections of these protrusions were subjected to *in situ* hybridization with probes specific for *Musashi*, which encodes a neural RNA-binding protein highly enriched in neural precursor cells (32), *Six3*, a homologue of *Drosophila* homeobox gene *sine oculis*, that is expressed in inner and outer nuclear layers (33), and *Rx*, a paired-class homeobox gene, which is expressed in the inner nuclear layer, presumably bipolar cells of the developing retina (34). Immunohistochemical staining with anti-Islet1 and anti-neurofilament antibodies was also performed (Fig. 4K). These analyses suggested that the tubular structures consist of well-differentiated retinal layers, which include nerve fibres, ganglion cells and developing inner and outer nuclear layer cells, with an outer surface layer of nerve fibres and an inner surface of photoreceptor cells. These tubular and fold structures suggest that the horizontal overgrowth of the neural retinal layer occurred at the regions where Pax6(+5a) was misexpressed. As space was limited even in the enlarged eyeball, the regional expansion of the cells seemed to push the retinal layer up into the vitreous cavity. Such drastic outgrowths that contain all retinal cell types was never obtained when Pax6(−5a) was misexpressed. Electroporation of the empty vector alone or the pCAGGS-GFP or both constructs did not induce any phenotypic changes. Thus, we conclude that the Pax6(+5a) isoform can induce horizontal overgrowths of the retina that protrude into the vitreous cavity. Of the 187 treated eyes, 34% of the Pax6(+5a)-treated eyes, which showed protrusion of the retina, became significantly larger than untreated control eyes (Fig. 4F). Although we have reproducibly generated this protruding retina by electroporating at HH stages 16–24, such morphological alterations were not induced when the electroporation was performed at later stages. Transduction of Pax6(−5a) or Pax6(+5a) using an adenoviral vector or electroporation using smaller amounts of plasmid DNAs caused similar, although somewhat weak phenotypic changes (data not shown). The incidence of the Pax6(−5a)- and Pax6(+5a)-dependent eye architectural changes at each stage is available in Supplementary Material.

We next examined the distribution of photoreceptor cells in the protruding retinal structures. Embryos were allowed to develop just before hatching (HH stages 40–45) and then analyzed. Some lectins, including peanut agglutinin and wheat germ agglutinin, specifically stain cone photoreceptor cells (35), which are normally condensed at the visual streak in the posterior portion of the chick eye (Fig. 5A and B e region). Histochemical examination revealed that the cone cells were detectable in the folded retina not only near the visual streak (d region) but also in the peripheral portion (c region) where lectin-staining is normally negative as observed in an unaffected peripheral portion (b region). Colour opsins are components of cone cells (2,3,36). RT–PCR showed that three types of colour *opsins* were expressed in the peripheral and posterior portions of the folded retina (c and d regions) at a similar level as in an unaffected region in the posterior portion of the retina (e region), and more intensely than an unaffected region of the peripheral portion of the retina (b region) (Fig. 5D). In contrast, the expression level of *rhodopsin*, a component of rod cells, was high in the peripheral areas and low in the visual streak (2,3). The peripheral portion of the folded retina (c region) exhibited *rhodopsin* expression at a similar level as the control peripheral area, whereas the expression level in the affected region in the posterior portion of the retina (d region) was similar to that in the visual streak (e region). These results suggest that the differentiation of retinal cells is highly promoted in the protruding retina to the level seen in the visual streak with regard to both the layer structure and the density of cone cells.

Effect of missense mutations of the *Pax6* gene on retinal overgrowth

To understand which element or structure of Pax6 is important for inducing the retinal overgrowth observed, we introduced several mutations into the Pax6 PD: (a) the R26G mutation in the NTS (25), (b) the R128C mutation in the CTS (4) or (c) the V54D mutation in exon 5a (5). The transactivation potentials of wild-type and mutant Pax6 with or without exon 5a have been assayed previously (5,22) or in this study using reporter genes containing P6CON or 5aCON, which are consensus binding sites for the (−5a) and (+5a) isoforms,

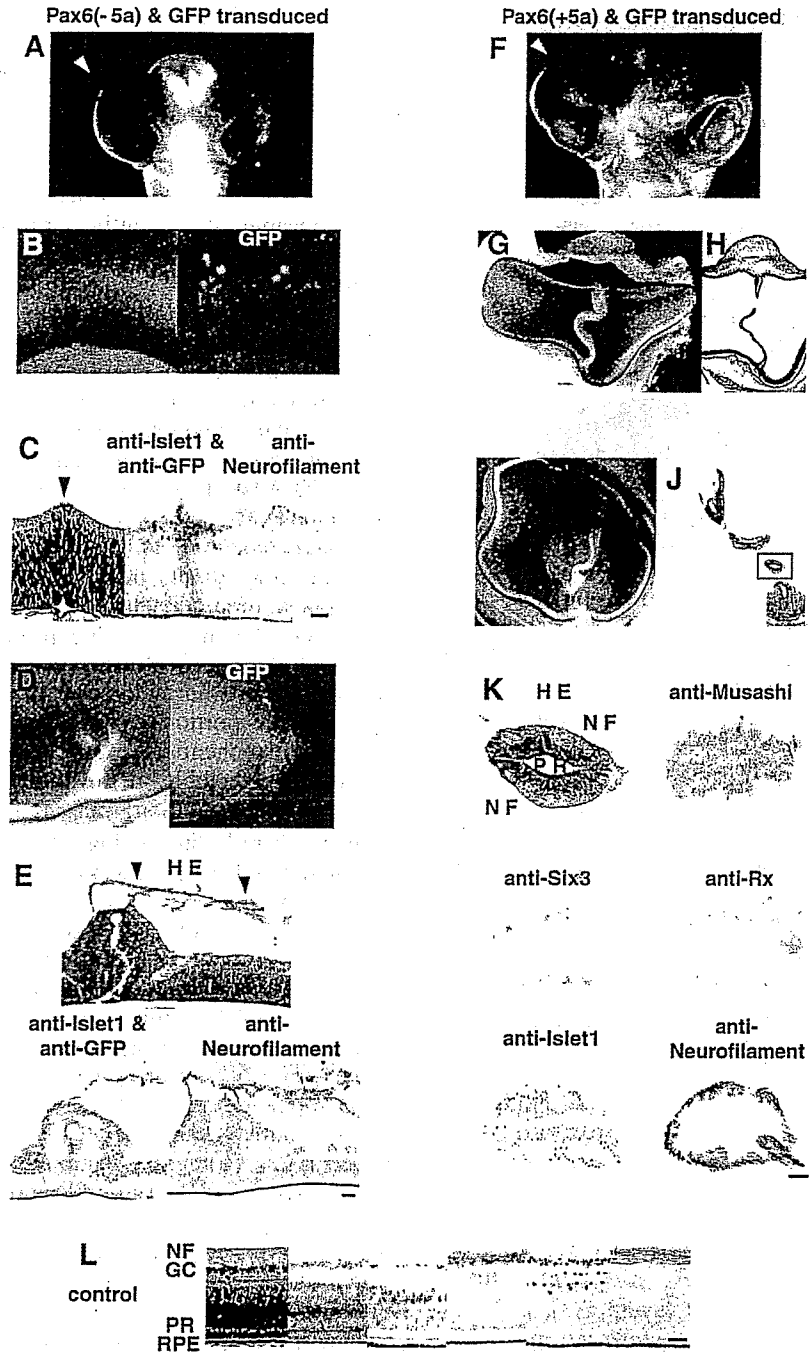

Figure 4. Later changes in the developing chick eye induced by electroporation of Pax6(−5a) (A–E) or Pax6(+5a) (F–K) together with GFP. (A–C) A Pax6(−5a)-transduced embryo at HH stage 30. (A) The frontal view shows an enlarged eye (arrowhead). (B) The inside views show several areas of swelling on the retinal layer with green fluorescence (the right panel, matched field). (C) Sections stained with HE, anti-islet1, anti-GFP and anti-neurofilament antibodies. Islet1 (brown) and GFP (violet) were double-stained. Ganglion cells (arrowhead) excessively differentiated in the surface layer of the thickened retina where the electroporated GFP constructs is expressed (bar scale 20 μm). (D, E) A Pax6(−5a)-transduced embryo at HH stage 34. (D) A view of the split eyeball shows embankment-like swelling from the retina with numerous fibres with green fluorescence (matched field). (E) Numerous fibres grow from the embankment-like retina into the vitreous cavity (arrowheads). Sections immunostained with anti-Islet1 (brown), anti-GFP (violet in the left lower panel) and anti-neurofilament (brown) antibodies show expression of the electroporated constructs and ectopic growth of the nerve bundles from the retina (bar scale 20 μm). (F–H) A Pax6(+5a)-transduced embryo at HH stage 34. (F) A frontal view shows a significantly enlarged eye that breaks through the eyelid skin (arrowhead). Views of the split eyeball (G) and section with HE staining (H) show that the retina overgrows to show fold structure. (I–K) A Pax6(+5a)-transduced embryo at HH stage 36. Views of the split eyeball (I) and section with HE staining (J) show that the retina overgrows into stick structure. GFP expression was weak and could not be detected in the aberrantly growing tissues. (K) Analysis of the boxed region of the section indicated by (J) by *in situ* hybridization using probes specific for *Musashi*, *Six3* and *Rx* and immunohistochemistry with anti-Islet1 and anti-neurofilament antibodies. These analyses suggest that the aberrantly growing tissues in the Pax6(+5a)-transduced eyes are composed of well-differentiated retina layers (bar scale 20 μm). NF, nerve fibres; PR, photoreceptors. (**L**) A portion of the posterior retina normally developing at a corresponding stage is illustrated for comparison. From the left to right panel: ME, anti-Musashi, anti-Six3, anti-Rx, anti-Islet1, anti-neurofilament. NF, nerve fibres; GC, ganglion cells; PR, photoreceptors; RPE, retinal pigment epithelium (bar scale 20 μm).

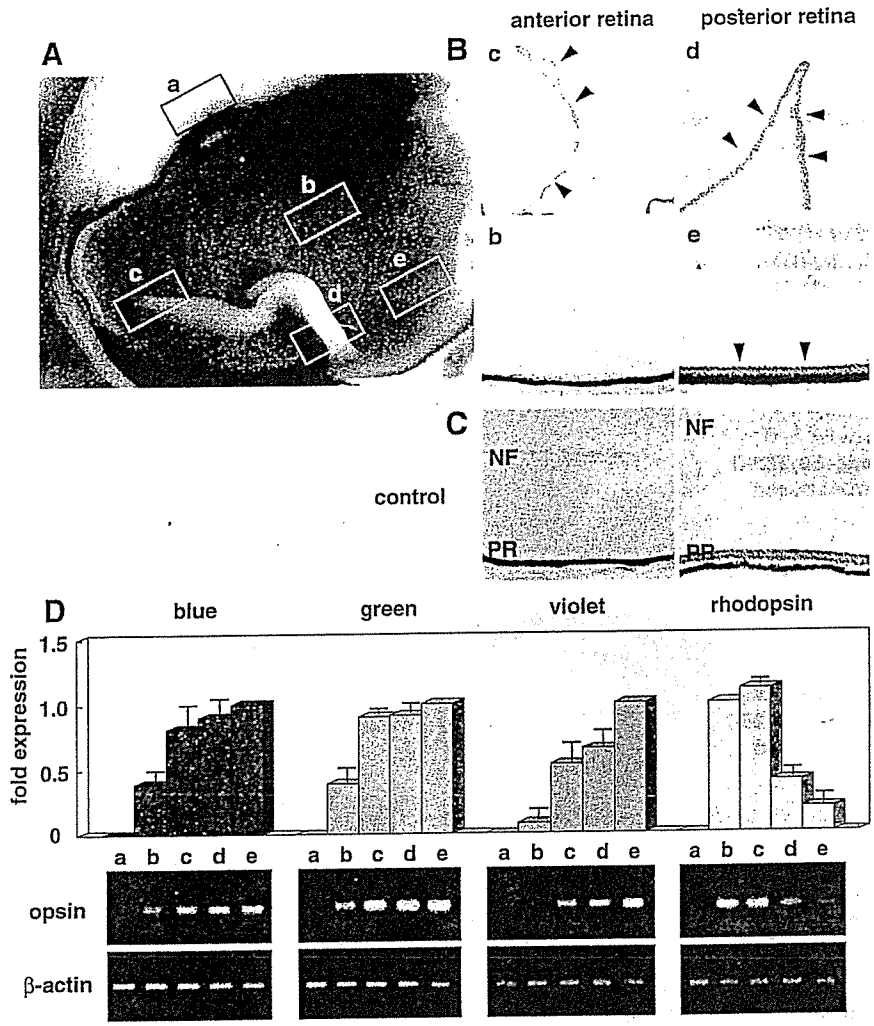

Figure 5. Differentiation of photoreceptor cells in the extruding and folded retina induced by electroporation of Pax6(+5a) at HH stage 18. (**A**) A view of a split eyeball at HH stage 45 shows the folded retina. Five areas were examined: (a) the cornea, (b) an unaffected region in the peripheral portion of the retina, (c) a peripheral portion of the folded retina, (d) a posterior portion of the folded retina and (e) an unaffected region in the posterior portion of the retina including the visual streak. (**B**) Staining with peanut agglutinin shows the presence of cone photoreceptor cells in the c region as well as in the d and e regions (arrowheads). (**C**) A portion of the retina normally developing at a corresponding stage is also illustrated for comparison. NF, nerve fibres; PR, photoreceptors (bar scale 20 μm). (**D**) Semi-quantitative RT–PCR demonstrates the expression of three colour *opsins* (*blue, green* and *violet*) and *rhodopsin* in the various regions. The bar graphs are shown as mean ± SD ($n = 3$) of ratio of expression in a–d region to that in e region (*blue, green* and *violet opsins*), or ratio of expression in a or c–e region to that in b region (*rhodopsin*). The photograph of RT–PCR analysis under the bar graph is representative of three independent experiments using six treated eyes.

respectively. As summarized in Figure 6A, the NTS in Pax6(−5a) wild-type is responsible for P6CON-binding, while in Pax6(+5a) wild-type, the insertion of 14 amino acids encoded by exon 5a into the NTS abolishes its NTS P6CON-binding activity and unmasks the CTS 5aCON-binding ability. The R26G mutation in the NTS strongly impairs the NTS- and P6CON-mediated transcriptional activation of Pax6(−5a) and increases the CTS- and 5aCON-mediated transcriptional activation of Pax6(+5a). In contrast, the R128C mutation in the CTS abolishes the CTS- and 5aCON-mediated transcriptional activation of Pax6(+5a), and hyperactivates the NTS- and P6CON-mediated transcription activation of Pax6(−5a). The V54D mutation in exon 5a has a weak inhibitory effect on the CTS-and 5aCON-mediated transcriptional activation, but increases the NTS- and P6CON-mediated transcriptional activation. Thus, it has been proposed that the two subdomains negatively regulate each other, and exon 5a thus appears to function as a molecular switch that determines target gene specificity. When these mutants were misexpressed in the primordial retina of HH stages 16–30 chick embryos, only Pax6(+5a) R26G and Pax6(−5a) R128C induced a phenotypic change. Retinal overgrowth was observed in 34% and 26% of the eyes that had received Pax6(+5a) R26G ($n = 54$) and Pax6(−5a) R128C ($n = 56$) respectively, although the observed phenotypic changes were less significant than those induced by the respective wild-type Pax6 isoforms. Morphological changes induced by Pax6(+5a) R26G were more drastic than those induced by Pax6(−5a) R128C. Retinal swelling and string- and stick-like structures induced by Pax6(+5a) R26G (Fig. 6B), and

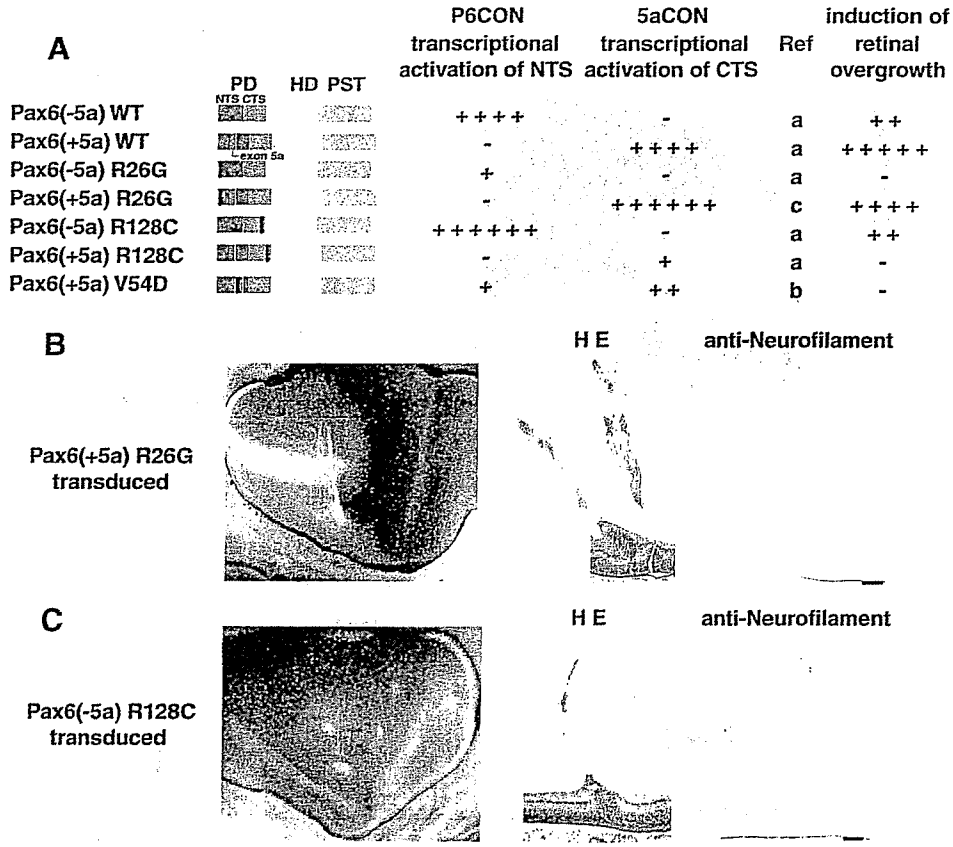

Figure 6. Effect of missense mutations of the *Pax6* gene on retinal overgrowth. (**A**) Schematic structure of the Pax6 wild-type and mutant (R26G, R128C and V54D) proteins with or without exon 5a that were used in this study. Our *in vitro* functional assays using P6CON- and 5aCON-CAT reporters in P19 cells have been reported previously [a, Yamaguchi *et al.* (22); b, Azuma *et al.* (5)] or are reported for the first time in this study (c). The effects of the mutants on overgrowth of the retina are also summarized. PD, paired domain (red, NTS; purple, CTS; blue, exon 5a; black bar, missense mutation); HD, homeodomain; PST, proline–serine–threonine rich transactivating domain. Each of the Pax6 mutants was electroporated into the right eye of HH stage 16 chick embryos and the changes around HH stage 35 were observed. (**B**) An eye that misexpresses Pax6(+5a) that carries the R26G mutation. The split eyeball shows the string- or stick-like structure of the overgrowing retina (left panel) (Pe, the pecten). Sections stained with HE and anti-neurofilament antibody suggest that the overgrowing tissues are thick bundles of nerve fibre and immature retina tissues (right panels, bar scale 100 μm). (**C**) An eye that misexpresses Pax6(−5a) that carries the R128C mutation. The split eyeball shows areas of swelling on the retina with fine fibres (left panel). Sections stained with HE and anti-neurofilament antibody reveal excessive differentiation of ganglion cells and their nerve fibres (right panels, bar scale 100 μm).

fibres induced by Pax6(−5a) R128C (Fig. 6C) are shown as examples. The incidence of eye architectural changes by transduction of each mutant at each developmental stage is available in Supplementary Material.

DISCUSSION

We have shown here that when Pax6 is overexpressed in the developing chick eye, it induces ectopic differentiation of the retina. Compared with the effect of Pax6(−5a), Pax6(+5a) induces a remarkable artificial retina-like structure. Intriguingly, the ectopic retina-like structure induced by Pax6(+5a) is highly differentiated and contains well-formed retinal layers that express cone-specific colour opsins. We believe that the retinal overgrowth reported here is not an artifact but rather an exaggeration of the natural role of Pax6(+5a) in retinal development, namely, in the formation of the retinal area where visual cells highly accumulate. The assumption is based on two lines of evidence, as described subsequently.

First, Pax6(+5a) is expressed in a region of the developing retina where visual cells are densely packed (Figs 1 and 2). Previous studies have revealed that Pax6(+5a) is abundantly expressed in the lens and iris (37,38), but the expression pattern of Pax6(+5a) in the retina has not been clarified. As shown in previous studies and in the study reported here, the expression of the two Pax6 isoforms in the developing eye seems highly regulated at the levels of transcription and mRNA splicing (39,40).

Secondly, there is a clear correlation between the mutations in Pax6(+5a) that are associated with abnormal foveal formation in humans and that affect ectopic retinal formation in chick embryos. The V54D and R128C mutations disturbed the ectopic retinal structures induced by Pax6(+5a) as shown in Figure 6, while previous genetic analyses showed that these mutations are associated with foveal hypoplasia in human patients (4,5,26). As the V54D mutation in exon 5a should not affect the structure of Pax6(−5a), these observations suggest that Pax6(+5a) probably plays an important role in the formation of the fovea. Curiously, the V54D

mutation had only a modest effect on the transactivation activity of Pax6(+5a) in our reporter assay using P19 cells. It may be that a putative retina-specific cofactor that is not expressed in P19 cells may regulate the Pax6(+5a) activity in a V54D mutation-sensitive manner, thereby causing the apparent discrepancy. Alternatively, the V54D mutation may show a more potent effect when *cis* elements that diverge from the consensus sequences are used.

The two Pax6 isoforms seem to function differently in a qualitative rather than quantitative fashion. Pax6(−5a) overexpression does induce ectopic retina-like tissues. However, the incidence is far lower and the structures induced are far more immature when compared with those induced by Pax6(+5a) overexpression. As shown in Figure 6, the R26G mutation in the NTS and the R128C mutation in the CTS selectively impaired the induction of aberrant retinal structures by Pax6(−5a) and Pax6(+5a), respectively. Previous *in vitro* assays showed that Pax6(−5a) and Pax(+5a) bind to the distinct consensus sequences P6CON and 5aCON via different DNA-binding domains, namely, the NTS and the CTS, respectively. Thus, it is very likely that Pax6(−5a) and Pax6(+5a) have a different structural requirement for retinal development independently of each other and via different mechanisms. As these experiments were done in the retina that has endogenous Pax6 proteins, however, there is also a possibility that Pax6(+5a) exerts its effect on retinal development through modulation of Pax6(−5a) activity.

A different mechanism for Pax6-mediated gene regulation has been identified in *D. melanogaster* (41). There are four Pax6-related genes in *Drosophila*, namely *eyeless, twin of eyeless, eyegone* and *twin of eyegone.* Among them, *eyegone* has strong structural similarity with Pax6(+5a) and has been linked to growth control in the *Drosophila* eye. Overexpression of human Pax6(+5a) but not of Pax6(−5a) in *Drosophila* larvae induces strong overgrowth. Similarity of eyegone and Pax6(+5a) at a functional level is indicated by our data showing that overexpression of human Pax6(+5a) induces strong overgrowth of retina in the vertebrate eye.

Recently, mice lacking the Pax6(+5a) isoform were shown to have iris hypoplasia (38). Thus, the iris may be another part of the eye that is controlled by the Pax6(+5a) isoform. However, the knock-out mice showed no apparent abnormality in the retina. This does not conflict with our data, however, because mice intrinsically lack areas of high dense visual cells, including the fovea.

The regional expression of Pax6(+5a) may also be related to eyeball structure. It has been reported that a strictly controlled level of Pax6 expression is critical for the normal development of eyes. Transgenic mice carrying multiple copies of the Pax6 gene manifest severe eye anomalies and microphthalmos (42), while the same abnormalities are observed in mice with haploinsufficiency of this gene (43). However, microphthalmos is often associated with eye anomalies in which numerous eye tissues are affected (44,45). As Pax6 is expressed in numerous eye tissues throughout development (15–17), it may be that in the transgenic mice, the eye tissues, each of which expresses an abnormal dose of the gene (either loss-of-function or gain-of-function), affect neighbouring tissues and disturb their mutual relationship in eyeball growth, resulting in microphthalmos. In contrast, *in ovo* electroporation is able to transfer genes to a selected tissue. In our experiment, overexpression of Pax6 in the chick retina primordium caused enlarged eyes. The outer coat of the eyeball corresponding to areas of Pax6(+5a) misexpression was prominently enlarged. It is thought that retinal growth influences eyeball growth (1,45), and that the accumulation of retinal cells in the temporal posterior area may cause a larger growth in the temporal side of the eyeball than in the nasal side. Regional expression of the Pax6(+5a) isoform in the temporal posterior retina may lead to eyeball asymmetry.

Our observations also have implications regarding phylogenic development. The retinal layer structures are much more complex in vertebrates than in invertebrates. Structures that caused the visual cells to congregate at high density, such as the fovea, area centralis and visual streak, and eyeball asymmetry first appeared in fishes (1–3). The splice variant of Pax6 with exon 5a is present in vertebrates but not in invertebrates (20,21,38) except for *Drosophila*, which has *eyegone*, a putative homologue of Pax6(+5a) (42). Therefore, the acquisition of the Pax6 splice variant during evolution may have contributed to the formation of highly organized eye architectures that yield better vision. Thereafter, vertebrates may have preserved exon 5a so that they could form a restricted retinal domain that has high visual acuity.

The mechanism that regulates Pax6 alternative splicing has not yet been elucidated. Areas where retinal cells accumulate, including the visual streak, area centralis, and fovea, are positioned to promote visual acuity among animal species. Thus, further studies should focus on the signalling molecules that regulate the expression of Pax6 isoforms. In reproductive medicine research, studies have focused on transferring transcriptional factors into stem cells (46). As Pax6 induces the ectopic formation of eyes in flies (13) and frogs (14), this gene may be useful for regenerating regional eye tissue in vertebrates as well. Our results indicate that the use of Pax6(+5a) may be more suitable than Pax6(−5a) for reproducing highly differentiated retinal structures.

MATERIALS AND METHODS

Immunohistochemistry and *in situ* hybridization

A monoclonal antibody against chicken Pax6 that reacts to both Pax6(−5a) and Pax6(+5a) in chicken, monkey and human tissues has been described previously (16,17). A polyclonal antibody against the 14 amino acid residues encoded by exon 5a (THADAKVQVLDNQN) was raised by immunizing New Zealand white rabbits with a synthetic peptide. After purification, the immunoreactivity of the antibody was confirmed by ELISA and its specificity was further assayed by western blotting (data not shown). Antibodies against GFP (Clontech), 5-bromo-2′-deoxyuridine (BrdU; DAKO), Islet-1 protein (DSHB), Chx10 protein (Exalpha Biologicals), neurofilament H (DAKO) and peanut agglutinin (Vector) were purchased. Specimens were fixed in 4% paraformaldehyde, embedded in a Tissue-Tek OCT compound (Sankyo, Tokyo), and cryo-sliced into 8 μm sections. The sections were stained with haematoxylin and eosin (HE), or with a specific antibody followed by visualization with peroxydase

and diaminobenzidine. Section *in situ* hybridization was performed as described (47). Probes were prepared from plasmids that contain chick *Musashi* (*Eco* RI, *T7* polymerase), *Six3* (*Hin*dIII, *T3*) and *Rx* (*Hin*dIII, *T3*).

RNA isolation and RT–PCR

Total RNA was isolated from tissues excised from one to five chick embryos using an RNeasy Mini Kit (Qiagen) and converted to cDNA by a standard procedure using SuperScript II reverse transcriptase and adapter primers (GibcoBRL). cDNA was amplified under nonsaturating PCR conditions using the following primer sets: chicken *Pax6*, 5′-CGGCAG AAGATCGTGGAACTCG and 5′-GCACTCTCGTTTATA CTGCGCTAT [this yields a 207 bp band for *Pax6(−5a)* and a 249 bp band for *Pax6(+5a)*]; chicken *blue opsin*, 5′-GGCCTTTATGTTCCTCCTCATCG and 5′-CAGATGA CGAGGAAGCGCTCGA (297 bp); *green opsin*, 5′-TCCCT GGTGGTCTTGGCCATAG and 5′-TGCCTCTCGGACTTT GCAGATGA (320 bp); *violet opsin*, 5′-CTACCTACAG ACGGCCTTCATG and 5′-GCAGATAACGATGTAACG CTCGA (310 bp); and *rhodopsin*, 5′-GGCTGCCTACAT GTTCATGCTGA and 5′-ACGGCCAGGACGACGAGT GAC (281 bp). The PCR products were separated by gel electrophoresis. To standardize the RNA amounts, *β-actin* was also amplified by PCR with its specific primers: 5′-GT GGGTCGCCCCAGACATCA and 5′-CTCCTTGATGTCAC GCACAATTTC (540 bp). The PCR amplication involved 30 cycles of 94°C for 1 min, 60°C for 1 min and 72°C for 2 min. It should be noted that the alternative splicing exon of the human and mouse *Pax6* genes is situated between exon 5 and 6 and is known as 5a. However, the *Pax6* gene structure of the chick strain we used has not yet been fully determined. It may be that the alternative splicing exon of the chick may later be designated differently. For example, it has been suggested that this exon in the quail *Pax6* gene should be denoted as exon 4a. Nevertheless, in this report, we employ the term 5a to indicate the alternative splicing exon in the chick *Pax6* gene.

In ovo electroporation

Expression plasmids [pCAGGS-PAX6(−5a) and pCAGGS-PAX6(+5a)] carry the entire human *PAX6* coding region with or without exon 5a under the control of a cytomegalovirus enhancer and chicken β-actin promoter (5,22). The mutant forms of PAX6 expression plasmid were generated by PCR-based *in vitro* mutagenesis (5,22,27). Fertilized eggs of a domestic chick strain were purchased from Nisseizai (Tokyo). A small window was opened for access, and phosphate buffered saline was poured over the embryo to obtain appropriate resistance. The eggs were injected with ∼0.1 μl of the DNA solution that contains an expression construct for GFP (pCAGGS–GFP) and one of the Pax6 expression plasmids (5 mg/ml) together with a fastgreen dye. The dye confirms that the injection was correctly targeted. Eggs, in which early changes are examined, were also injected with BrdU (0.3 mg/ml). The DNA solution was either injected into a region that is close to the primitive retina in the right optic cup or directly into the retina of the right eye of the embryos with a sharp glass pipette. The head of the embryo was then placed between platinum electrodes and electric pulses were applied (25–40 V, 90 ms, one to six times) with a CUY 21 electroporator (BEX Co., Tokyo). The egg-shells were sealed and the embryos were allowed to develop in humidified incubators at 38°C.

SUPPLEMENTARY MATERIAL

Supplementary Material is available at HMG Online.

ACKNOWLEDGEMENTS

We thank Drs H. Fujisawa (Nagoya University) and Y. Tanioka (Central Institute for Experimental Animals) for providing antibodies and marmoset specimens, respectively. We also thank Ms K. Saito for manuscript preparation. This study was supported in part by Grants for Genome, Tissue Engineering Biotechnology, for Sensory and Communicative Disorders, and for Paediatric Researches from the Ministry of Health, Labour and Welfare, Japan, and in part by a Grant for Organized Research Combination System from the Ministry of Education, Culture, Sports, Science and Technology, Japan.

REFERENCES

1. Duke-Elder, S. (1958) The eye in evolution. In *System of Ophthalmology*, Henry Kimpton, London, Vol. 1.
2. Rodieck, R.W. (1998) *The First Step of Seeing*. Sinauer, Sunderland.
3. Oyster, C.W. (1999) *The Human Eye*. Sinauer, Sunderland.
4. Azuma, N., Nishina, S., Okuyama, T., Yanagisawa, H. and Yamada, M. (1996) PAX6 missense mutation in isolated foveal hypoplasia. *Nat. Genet.*, **13**, 141–142.
5. Azuma, N., Yamaguchi, Y., Handa, H., Hayakawa, M., Kanai, A. and Yamada, M. (1999) Missense mutation in the alternative splice region of the *PAX6* gene in eye anomalies. *Am. J. Hum. Genet.*, **65**, 656–663.
6. McCabe, K.L., Gunther, E.C. and Reh, T.A. (1999) The development of the pattern of retinal ganglion cells in the chick retina: mechanisms that control differentiation. *Development*, **126**, 5713–5724.
7. Marquardt, T., Ashery-Pedan, R., Andrejewski, N., Scardigli, R., Guillemot, F. and Gruss, P. (2001) Pax6 is required for the multipotent state of retinal progenitor cells. *Cell*, **105**, 43–55.
8. Sharon, D., Blackshaw, S., Cepko, C.L. and Dryja, T.P. (2002) Profile of the genes expressed in the human peripheral retina, macula, and retinal pigment epithelium determined through serial analysis of gene expression (SAGE). *Proc. Natl Acad. Sci. USA*, **99**, 315–320.
9. Gehring, W.J. (1996) The master control gene for morphogenesis and evolution of the eye. *Genes Cells*, **1**, 11–15.
10. Callaerts, P., Halder, G. and Gehring, W.J. (1997) PAX-6 in development and evolution. *Annu. Rev. Neurosci.*, **20**, 483–532.
11. Ashery-Padan, R. and Gruss, P. (2001) Pax6 lights-up the way for eye development. *Curr. Opin. Cell Biol.*, **13**, 706–714.
12. Chi, N. and Epstein, J.A. (2002) Getting your Pax straight: Pax proteins in development and disease. *Trends Genet.*, **18**, 41–47.
13. Halder, G., Callaerts, P. and Gehring, W.J. (1995) Induction of ectopic eye by targeted expression of the eyeless gene in *Drosophila*. *Science*, **267**, 1788–1792.
14. Chow, R.L., Altmann, C.R., Lang, R.A. and Hemmati-Brivanlou, A. (1999) *Pax6* induces ectopic eye in a vertebrate. *Development*, **126**, 4213–4222.
15. Walther, C. and Gruss, P. (1991) *Pax6*, a murine paired box gene, is expressed in the developing CNS. *Development*, **113**, 1435–1449.
16. Kawakami, A., Kimura-Kawakami, M., Nomura, T. and Fujisawa. H. (1997) Distributions of PAX6 and PAX7 proteins suggest their involvement in both early and late phases of chick brain development. *Mech. Dev.*, **66**, 119–130.

17. Nishina, S. Kohsaka, S., Yamaguchi, Y., Handa, H., Kawakami, A., Fujisawa, H. and Azuma, N. (1999) PAX6 expression in the developing human eye. *Br. J. Ophthalmol.*, **83**, 723–727.
18. Czerny, T., Schaffner, G. and Busslinger, M. (1993) DNA sequence recognition by Pax proteins: bipartite structure of the paired domain and its binding site. *Genes Dev.*, **7**, 2048–2061.
19. Xu, W., Rould, M.A., Jun, S., Despan, C. and Pabo, C.O. (1995) Crystal structure of a paired domain-DNA complex at 25A resolution reveals structural basis for Pax developmental mutations. *Cell*, **80**, 639–650.
20. Epstein, J.A., Glaser, T., Cai, J., Jepeal, L., Walton, D.S. and Maas, R.L. (1994) Two independent and interactive DNA-binding subdomains of the Pax6 paired domain are regulated by alternative splicing. *Genes Dev.*, **8**, 2022–2034.
21. Epstein, J.A., Cai, J., Glaser, T., Jepeal, L. and Maas, R.L. (1994) Identification of a Pax paired domain recognition sequence and evidence for DNA-dependent conformational changes. *J. Biol. Chem.*, **269**, 8355–8361.
22. Yamaguchi, Y., Sawada, J., Yamada, M., Handa, H. and Azuma, N. (1997) Autoregulation of Pax6 transcriptional activation by two distinct DNA-binding subdomains of the paired domain. *Genes Cells*, **2**, 255–261.
23. Richardson, J., Cvekl, A. and Wistow, G. (1995) Pax-6 is essential for lens-specific expression of zeta-crystallin. *Proc. Natl Acad. Sci. USA*, **92**, 4676–4680.
24. Martha, A., Ferrell, R.E., Mintz-Hittner, H., Lyons, L.A. and Saunders, G.F. (1994) Paired box mutations in familial and sporadic aniridia predicts truncated aniridia proteins. *Am. J. Hum. Genet.*, **54**, 801–811.
25. Hanson, I., Fletcher, J.M., Jordan, T., Brown, A., Taylor, D., Adams, R.J., Punnett, H.H. and van Heyningen, V. (1994) Mutations at the *PAX6* locus are found in heterogeneous anterior segment malformations including Peters' anomaly. *Nat. Genet.*, **6**, 168–173.
26. van Heyningen, V. and Williamson, K.A. (2002) PAX6 in sensory development. *Hum. Mol. Genet.*, **11**, 1161–1167.
27. Azuma, N., Yamaguchi, Y., Handa, H., Tadokoro, K., Asaka, A., Kawase. E. and Yamada, M. (2003) Mutations of the *PAX6* gene detected in patients with a variety of optic nerve malformations. *Am. J. Hum. Genet.*, **72**, 1565–1570.
28. Itasaki, N., Bel-Vialar, S. and Krumlauf, R. (1999) 'Shocking' developments in chick embryology: electroporation and *in ovo* gene expression. *Nat. Cell Biol.*, **1**, E203–207.
29. Niwa, H., Inoue, S., Hirano, T., Matsuo, T., Kojima, S., Kubota, M., Ohashi, M. and Tsuji, F.I. (1996) Chemical nature of the light emitter of the Aequorea green fluorescent protein. *Proc. Natl Acad. Sci. USA*, **93**, 13617–13622.
30. Halfter, W. (1998) Disruption of the retinal basal lamina during early embryonic development leads to a retraction of vitreal end feet, an increased number of ganglion cells, and aberrant axonal outgrowth. *J. Comp. Neurol.*, **397**, 89–104.
31. Torelli, S., Sogos, V., Marzilli, M.A., D'Atri, M. and Gremo, F. (1989) Developmental expression of intermediate filament proteins in the chick embryo retina: *in vivo* and *in vitro* comparison. *Exp. Biol.*, **48**, 187–196.
32. Sakakibara, S. and Okano, H. (1997) Expression of neural RNA-binding proteins in the postnatal CNS: implications of their roles in neuronal and glial cell development. *J. Neurosci.*, **17**, 8300–8312.
33. Kawakami, K., Ohto, H., Takizawa, T. and Saito, T. (1996) Identification and expression of six family genes in mouse retina. *FEBS Lett.*, **393**, 259–263.
34. Mathers, P.H., Grinberg, A., Mahon, K.A. and Jamrich, M. (1997) The *Rx* homeobox gene is essential for vertebrate eye development. *Nature*, **387**, 603–607.
35. Hageman, G.S. and Kuehn, M.H. (1998) Biology of the interphotoreceptor matrix–retinal pigment epithelium–retina interface. In Marmor, M. and Wolfensberger, T.J. (eds), *The Retinal Pigment Epithelium*. Oxford University Press, New York, pp. 361–391.
36. Nathans, J., Thomas, D. and Hogness, D.S. (1986) Molecular genetics of human color vision: the gene encoding blue, green, and red pigments. *Science*, **232**, 193–202.
37. Jaworski, C., Sperbeck, S., Graham, C. and Wistow, G. (1997) Alternative splicing of Pax6 in bovine eye and evolutionary conservation of intron sequences. *Biochem. Biophys. Res. Commun.*, **240**, 196–202.
38. Singh, S., Mishra, R., Arango, N.A., Deng, J.M., Behringer, R.R. and Saunders, G.F. (2002) Iris hypoplasia in mice that lack the alternatively spliced Pax6(5a) isoform. *Proc. Natl Acad. Sci. USA*, **99**, 6812–6815.
39. Kumar, J.P. (2001) Signalling pathways in *Drosophila* and vertebrate retinal development. *Nat. Rev. Genet.*, **2**, 846–857.
40. Marquardt, T. and Gruss P. (2002) Generating neuronal diversity in the retina: one for all. *Trends Neurosci.*, **25**, 32–38.
41. Dominguez, M., Ferres-Marco, D., Gutierrez-Avino, F.J., Speicher, S.A. and Beneyto, M. (2004) Growth and specification of the eye are controlled independently by eyegone and eyeless in *Drosophila melanogaster*. *Nat. Genet.*, **36**, 31–39.
42. Schedl, A., Ross, A., Lee, M., Engelkamp, D., Rashbass, P., van Heyningen, V. and Hastie, N.D. (1996) Influence of *PAX6* gene dosage on development: overexpression causes severe eye abnormalities. *Cell*, **86**, 71–82.
43. Hill, R.E., Favor, J., Hogan, B.L., Ton, C.C., Saunders, G.F., Hanson, I.M., Prosser, J., Jordan, T., Hastie, N.D. and van Heyningen, V. (1991) Mouse small eye results from mutations in a paired-like homeobox-containing gene. *Nature*, **354**, 522–525.
44. Duke-Elder, S. (1964) Congenital deformities. In *System of Ophthalmology*, Henry Kimpton, London, Vol. 3, part 2.
45. Burmeister, M., Novak, J., Liang, M.Y., Basu, S., Ploder, L., Hawes, N.L., Vidgen, D., Hoover, F., Goldman, D., Kalnins, V.I. *et al.* (1996) Ocular retardation mouse caused by Chx10 homeobox null allele: impaired retinal progenitor proliferation and bipolar cell differentiation. *Nat. Genet.*, **12**, 376–384.
46. Haruta, M., Kosaka, M., Kanegae, Y., Saito, I., Inoue, T., Kageyama, R., Nishida, A., Honda, Y. and Takahashi, M. (2001) Induction of photoreceptor-specific phenotypes in adult mammalian iris tissue. *Nat. Neurosci.*, **4**, 1163–1164.
47. Koshiba-Takeuchi, K., Takeuchi, J.K., Matsumoto, K., Momose, T., Uno, K., Hoepker, V., Ogura, K., Takahashi, N., Nakamura, H., Yasuda, K. *et al.* (2000) Tbx5 and the retinotectum projection. *Science*, **287**, 134–137.

未熟児網膜症

東　範行　国立成育医療センター眼科

要旨

未熟児網膜症は，低出生体重児の管理の進歩に伴って，近年増加しており，重症例も多くみられるようになった．定期的な眼底検査を行い，病期分類をよく理解して，重症例を見逃がさないことが重要である．治療は中等度網膜症であれば光凝固を，網膜剥離が進行すればバックリングや硝子体手術を行う．

Key Words
未熟児網膜症
病期分類
光凝固
硝子体手術

はじめに

未熟児網膜症は発達途上の網膜血管が増殖する疾患で，重症であれば失明に通ずる．網膜血管は胎齢15週に視神経乳頭部に現れ，眼底を周辺部にむかって成長していく．血管が眼底の最周辺部まで達するのは満期の40週頃なので，発育途上で出生して急な環境変化があると，網膜血管は異常な方向に増殖する．したがって，網膜症の発現頻度や程度は血管成長が未熟であるほど高いが，ほかにも発病に関する多くの因子がある．未熟児網膜症は，NICUでの管理の進歩によって一時減少していたが，体重の少ない児が救えるようになって[1)2)]再度増加し，重症網膜症も多くみられるようになった[3)~5)]．

未熟児網膜症の進行と病期分類

未熟児網膜症の初期は，血管成長先端部の網膜内で血管芽細胞が増殖を始め，白い境界線を形成する（図1）．やがて境界線上やその後部で新生血管が発芽し，しだいに融合して硝子体腔内へ伸びていく（図2）．

眼底では乳頭は鼻側に位置しており，網膜血管が乳頭から周辺まで成長する距離は鼻側に比べて耳側が長いので，耳側のほうで網膜症がおこりやすい．さらに進行すると，網膜剥離がお

0386-9806/04/¥100/頁/JCLS

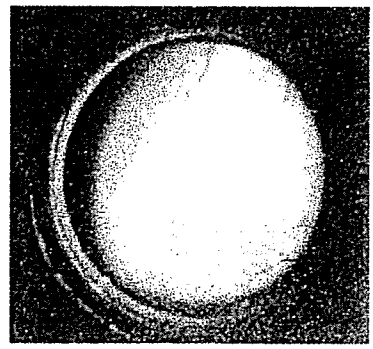

図1　境界線（眼底写真）

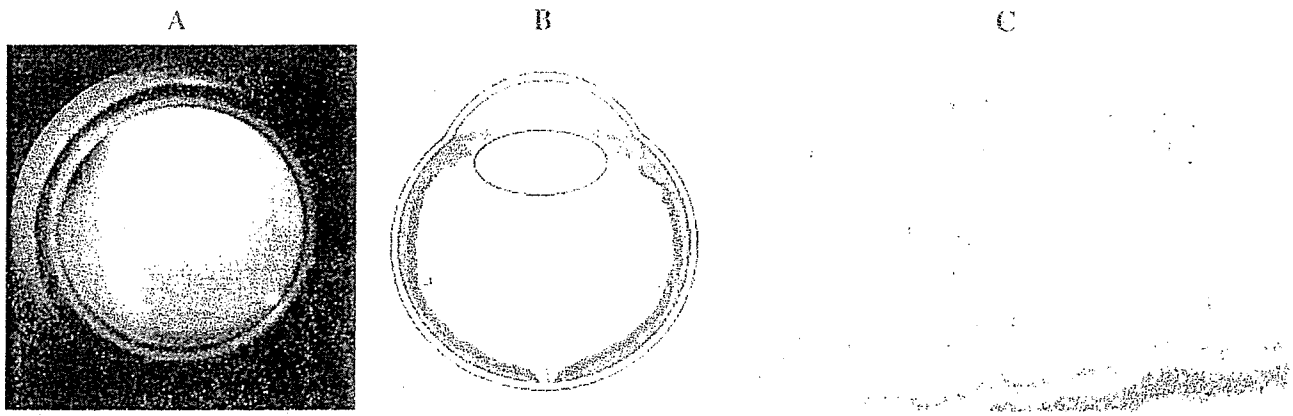

図2　発芽病変
A：眼底写真，B：眼球シェーマ，C：病理所見

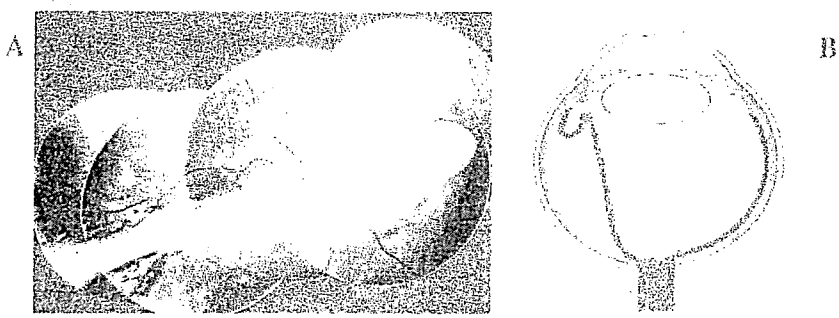

図3　網膜ひだ
A：眼底写真，B：眼球シェーマ

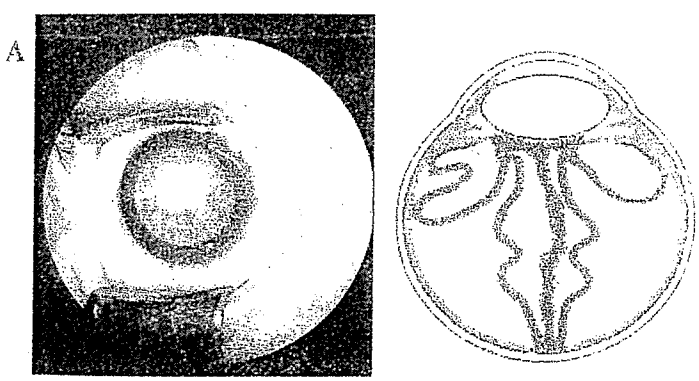

図4　白色瞳孔を示す高度な増殖による網膜全剝離
A：眼球前方の写真，B：眼球シェーマ

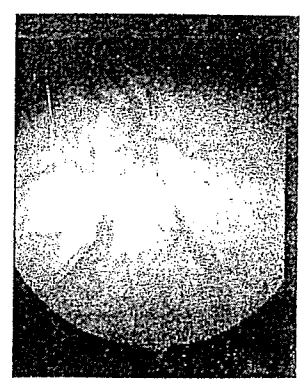

図5　Ⅱ型網膜症の後極血管の拡張と蛇行

こる．これは新生血管から形成された結合組織の収縮による牽引性剝離と，血管からの漏出による滲出性剝離の2種類がある．増殖組織が一側に限局していれば，網膜はそちらに引かれて伸展し，牽引乳頭や網膜ひだ（図3）を形成する．

高度な増殖がおこれば網膜は全剝離し，白色瞳孔を呈するようになる（図4）．ことに，網膜血管の成長が不良で拡張蛇行が強い場合は，短期間に進行して網膜全剝離になるおそれがある（厚生省分類Ⅱ型，図5）

この進行病期に関して，わが国では1976年に厚生省研究班によって『未熟児網膜症の診断ならびに治療基準』[6]が作成され，1983年には一

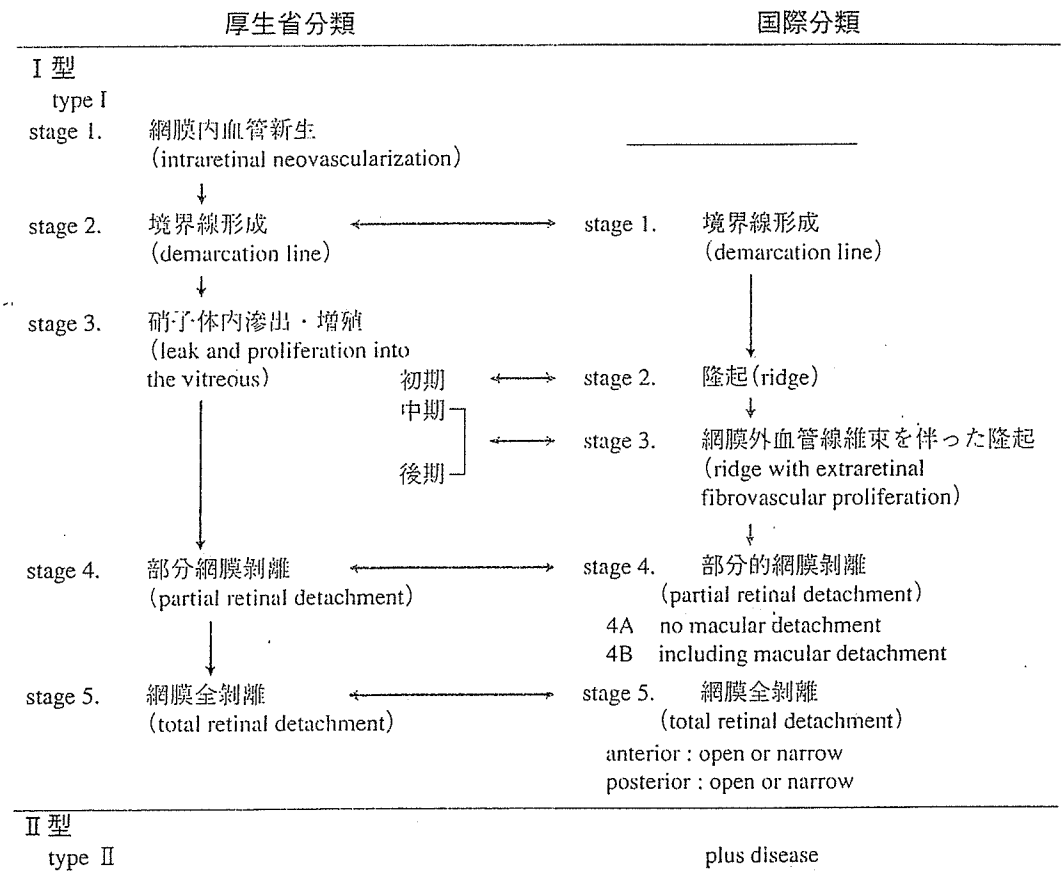

図6　厚生省分類と国際分類

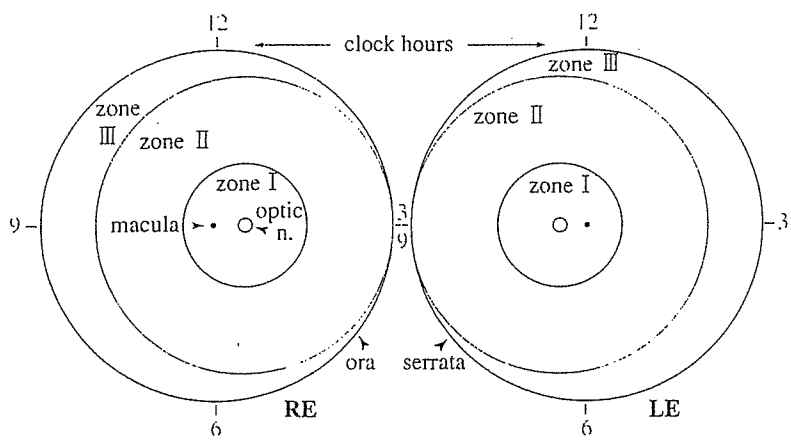

図7　国際分類の眼底 zone